Applied Physics B (2024) 130:79
https://doi.org/10.1007/s00340-024-08215-y

Applied Physics B
Lasers and Optics

RESEARCH

Study on the interaction of vertically structured double cavitation bubbles induced by pulsed laser

Qingmiao Ding[1] · Yunlong Shan[1] · Yanyu Cui[1] · Xiaoman Li[1] · Junguo Ni[1] · Junda Lv[2]

Received: 14 January 2024 / Accepted: 30 March 2024 / Published online: 21 April 2024

Abstract
Currently, the majority of research on double cavitation bubbles focuses on horizontally arranged structures, while investigations into the pulsation of vertically aligned double bubbles remain limited. This paper aims to conduct high-speed photography research on the interaction of vertically structured double cavitation bubbles induced by pulsed laser. The pulsed laser induced cavitation method is used to induce the formation of vertically arranged double cavitation bubbles, and high-speed photography techniques are employed to investigate their pulsation characteristics.The double cavitation bubbles studied are divided into three forms according to the initial size ratio S^*. The results indicate that, for vertically arranged double cavitation bubbles, similar-sized bubbles ($1 \leq S^* < 1.15$) exhibit mutual attraction and fusion, with a tendency for fusion preceding separation. Bubbles of different sizes ($1.15 \leq S^* < 3$) repel during the expansion process and attract during the shrinkage process.The pulsation of small bubbles with extremely different sizes ($S^* \geq 3$) is strongly influenced by repulsion, while the pulsation of large bubbles is essentially unaffected.

1 Introduction

The cavitation phenomenon refers to the occurrence of cavitation bubbles in a localized region of a liquid medium due to the deposition of energy, resulting in a change in temperature or pressure. When the change exceeds a certain threshold, the phenomenon of cavitation bubble formation occurs. On the one hand, the collapse of cavitation bubbles to form cavitation erosion has caused serious adverse effects on the material destruction of hydraulic machinery; on the other hand, the application of photo cavitation bubbles in the fields of bio-medicine, cavitation cleaning and strengthening has created huge Economic Value.Under different operating conditions and application scenarios, cavitation bubbles play distinct and crucial roles. Numerous studies have been conducted by previous scholars on the generation, growth, development, and collapse processes of cavitation bubbles, providing significant guidance for the practical applications of cavitation bubbles.However, the generation of cavitation bubbles often occurs in the form of cavitation clouds, cavitation bubble clusters, or gas pockets. The interactions among cavitation bubbles play a crucial role in their generation, growth, development, and collapse processes. Investigating the patterns of mutual influence among cavitation bubbles holds significant importance.

At this stage, the main methods for inducing cavitation include acoustic cavitation [1], spark-induced cavitation [2], laser-induced cavitation [3], etc. Acoustic cavitation typically utilizes ultrasonic waves as an energy source to induce cavitation. However, this method is generally employed for investigating the overall characteristics of cavitation phenomena from a macroscopic perspective. Ultrasonic-induced cavitation usually results in the formation of cavitation bubble clusters, characterized by a large quantity that is challenging to separate, making their properties complex [1]. Therefore, when generating a small quantity of cavitation

✉ Yanyu Cui
yycui@cauc.edu.cn

Qingmiao Ding
qmding@cauc.edu.cn

Yunlong Shan
shan18822286156@163.com

Xiaoman Li
lxmchh@outlook.com

Junguo Ni
19822073877@163.com

Junda Lv
ljdabc@126.com

[1] Civil Aviation University of China, Tianjin, China

[2] China National Aviation Fuel Supply Co Ltd, Beijing, China

bubbles, the latter two methods are usually employed. In comparison to spark-induced cavitation, the pulsed laser-induced cavitation method is simpler and easier to control. By adjusting laser parameters and optical paths, the size and initial position of cavitation bubbles can be controlled, offering advantages such as high precision, non-direct contact, and good symmetry in bubble generation [3]. As a result, the pulsed laser-induced method has gained widespread application. Since the 1970s, researchers have been focusing on the pulsation process of double cavitation bubbles, continually exploring the interactions and pulsation characteristics of these double cavitation bubbles. In 1973, Mitchell et al. [4] began to use high-speed cameras to record the interaction and dynamic process of two spark-induced cavitation bubbles. In 1985, Lauterborn et al. [5, 6] employed the pulsed laser-induced cavitation method to generate anti-phase double cavitation bubbles. They investigated the phenomena and formation mechanisms of anti-phase double cavitation bubble jets and vortices. In 1990, Tomita et al. [7] investigated the influence of relative size and relative position changes of two cavitation bubbles on the oscillatory behavior of double cavitation bubbles using the pulsed laser-induced cavitation method. In 2009, Fong et al. [8] employed electric spark-induced cavitation to generate two similarly sized bubbles and conducted a study on their pulsation behavior at different relative positions. They identified four pulsation behaviors of similarly sized bubbles: jetting toward each other, jetting away from each other, bubble coalescence, and a behavior termed the "catapult" effect. In 2009, P. A. Quinto-Su et al. [9] employed laser-induced cavitation to generate twin bubbles and recorded the dynamic changes of the two bubbles at different distances. They found that the interaction force between the double bubbles is inversely proportional to the distance between them. In 2011, Chew L W et al. [10] further extended the research into different-sized bubble domains. They used electric spark-induced cavitation to generate two bubbles of different sizes and investigated the influence of bubble size and phase on the jetting behavior between the two bubbles. In 2012, C.-T. Hsiao et al. [11] conducted numerical and analytical studies on the pulsation process of tandem double microbubbles between two parallel plates, optimizing the design of tandem-bubble control for biomedical applications such as in drug delivery and cell therapy. In 2015, Han Bing [12] conducted experimental and numerical simulation studies on the interaction of two laser-induced cavitation bubbles in bulk water. The research revealed that by adjusting the relative bubble positions, the time difference between bubble generation and the laser pulse energies determining the bubble sizes, the strength and direction of the emerging liquid jets can be controlled. This research Opened the door for systematic studies of jetting phenomena in multi-bubble systems and the reliable application of cavitation in medical technologies such as micropumping and opto-injection. In 2019, Tao Longbin et al. [13] investigated the complex pulsating process of multiple cavitation bubble coalescence, in which the fusion process of double cavitation bubbles was theoretically deduced and fitted. In 2020, Vicente Robles et al. [14] conducted an optimization study on the jet of two interacting laser-induced cavitation bubbles, analyzed the microjet effect on soft materials due to spatial and temporal separation in a double-bubble arrangement. They also quantified the advantageous targeting effectiveness of double cavitation bubbles over single cavitation bubble jetting for an agar gel-based skin phantom. In 2022, Fu Lei et al. [15] employed beam splitting of nanosecond pulsed lasers to induce the formation of two cavitation bubbles with similar dimensions. They conducted experimental studies on the fusion process of the bubbles at different intervals using high-speed cameras, bulk light scattering tests, and acoustic detection, elucidating the fusion pulsation process of double cavitation bubbles.

At present, both domestic and international research on the pulsation characteristics of single cavitation bubble has developed a relatively mature theoretical framework. However, there is still significant research space in the study of the pulsation characteristics of double cavitation bubbles. A limited amount of research has predominantly concentrated on horizontally aligned double cavitation bubbles, and the phenomena of mutual interaction between vertically aligned double cavitation bubbles in such structural arrangements remain incompletely discovered and explained. Compared with the horizontally aligned double cavitation bubbles, the two cavitation bubbles in the vertically arranged structure are in solution layers of different heights. Consequently, the external liquid pressure and buoyancy acting on the two bubbles are different. The pulsation characteristics of the cavitation bubble are affected by many factors, among which environmental pressure notably affects the cavitation time, pulsating expansion process, and collapse jet phenomenon of the bubble [16]. Therefore, the interaction between vertically aligned double cavitation bubbles theoretically presents a more complex and worthy of exploration phenomenon. This paper aims to investigate the pulsation characteristics of vertically aligned double cavitation bubbles generated by pulsed laser. By establishing a laser-induced cavitation experimental platform and employing pulsed laser induction methods along with high-speed photography techniques, we explore the coalescence and jetting processes of vertically structured double cavitation bubbles induced by pulsed laser. The results of this study hold important theoretical and practical significance for enhancing the understanding of pulsation characteristics and mutual interactions of double cavitation bubbles with different arrangements, better revealing the nature of the cavitation phenomenon, and promoting the practical application of cavitation.

2 Experimental methods

2.1 Experimental design

The experimental system for laser-induced cavitation is illustrated in Fig. 1. The experimental setup primarily consists of a computer control system, dual-pulsed solid-state laser, high-speed camera, LED light source, reflecting mirrors, focusing lens, three-dimensional positioning platform, and an acrylic tank. The experimental system employs a dual-pulsed solid-state laser as the excitation light source, using a 45 total reflection mirror aligned on the same optical axis as the excitation light source. A focusing lens is positioned directly beneath the reflective mirror for concentration, and the water tank is placed on a movable platform below the focusing lens. The pulsed laser, focusing lens, and three-dimensional positioning platform are all connected to the computer control system. The focal length of the focusing lens is 75 mm, and the three-dimensional positioning platform has a range of motion of ± 12.5 mm in both the X-and Y-axes and 10 mm in the Z-axis direction. The computer-linked controller controls the dual-pulsed solid-state laser to emit two laser beams with time intervals (adjustable in the range of 100 ns to 4000 ns in the experiment). The two laser beams are sequentially reflected by reflecting mirrors for total reflection and then focused by a focusing lens, and finally vertically incident into the water tank. Appropriately adjust the energy of the two laser beams (the laser energy range that generates larger cavitation bubbles in the experiment is adjusted between 140 and 180 mJ, and the laser energy range that generates smaller cavitation bubbles is adjusted between 60 and 160 mJ). When the laser energy exceeds the breakdown threshold of the liquid medium, breakdown occurs, leading to the formation of cavitation bubbles.During the experiment, a high-speed camera was used to record the dynamic process of the double cavitation bubbles in the water tank, and an LED light source was used to illuminate the cavitation area to assist in the shooting.

2.2 Experimental device

During the laser-induced cavitation experiment, professional instruments and equipment were used to conduct the experiment in an orderly manner, and to assist relevant detection equipment in measuring the experimental effect. Specific instruments include:

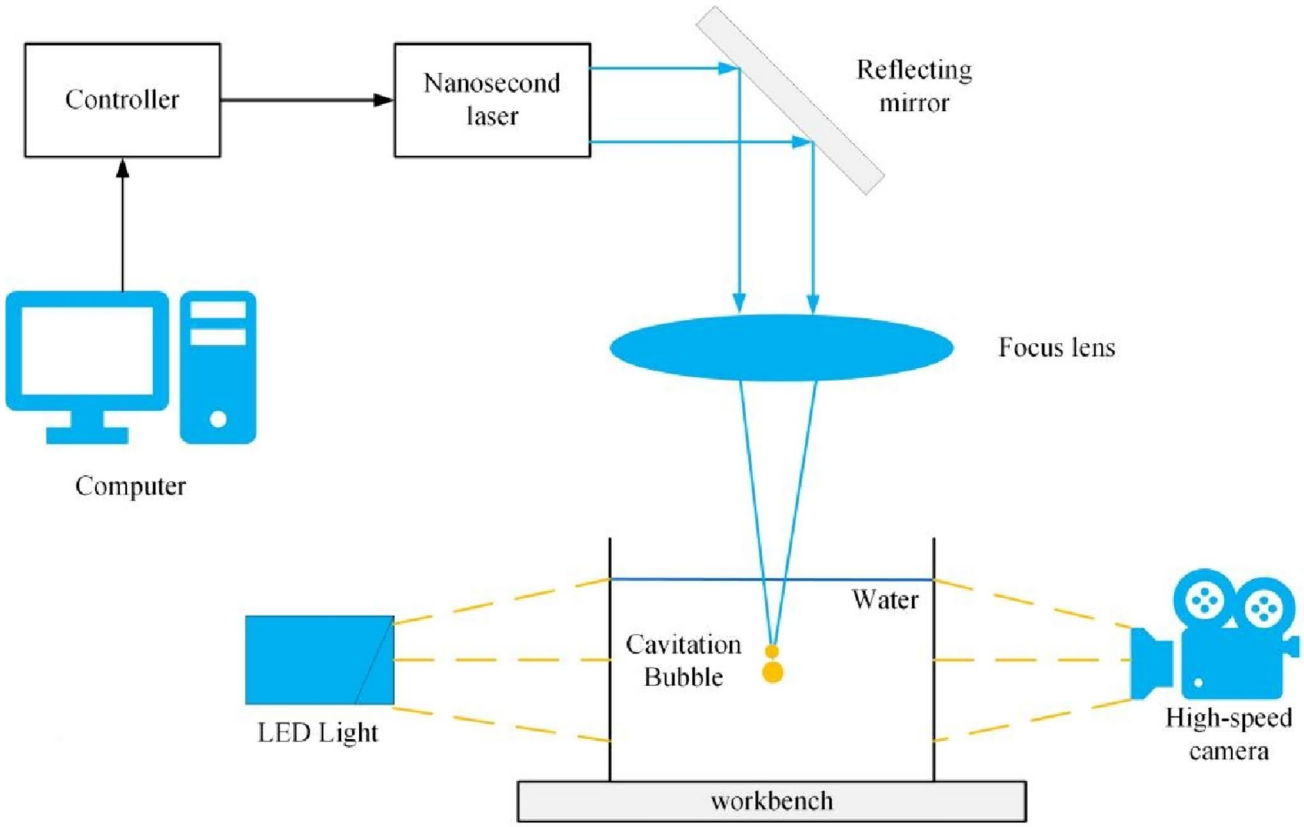

Fig. 1 Schematic diagram of laser induced double cavitation experimental device

a. Dual-pulsed solid-state laser

The dual-pulsed solid-state laser used in this experiment is a customized version of the Vlite-200, a high-energy dual-pulsed laser from the Vlite series produced by Beijing Beamtech Optronics Co., Ltd. It features a compact size, sturdy and durable structure, and high engineering sophistication. The laser parameters of the two segments of the dual-pulsed laser output can be independently adjusted. The output wavelength is customized to 1064 nm, with a repetition frequency ranging from 0 to 15 Hz, a pulse duration of 5–8 ns, and an adjustable output energy ranging from 20–200 mJ. By connecting to a computer control system, the time interval between the two pulses of the output laser can be adjusted from 100 to 4000 ns. The beam diameter of the output laser is 7 mm, with a divergence angle of less than or equal to 3 mrad.

b. high speed camera

The high-speed camera used in this experiment is Phantom VEO 1310 high-speed camera. The shooting speed in this experiment is 80,000 frames per second, with an image exposure time of 2 μs, and a resolution of 320 × 168.

c. LED light source

The cavitation area lighting in this experiment uses an RF always-on, flicker-free LED cold light source with a power of 200W.

2.3 Experimental program

This section first introduces two dimensionless parameters: the initial size ratio (S^*) and the relative distance (D^*). The initial size ratio (S^*) is defined as the ratio of the initial radius of the larger bubble to the initial radius of the smaller bubble.

$$S^* = \frac{R_{L0}}{R_{S0}} \tag{1}$$

The relative distance (D^*) is defined as the ratio of the initial center-to-center distance between two bubbles to the sum of the initial radii of the two bubbles.

$$D^* = \frac{L}{R_{L0} + R_{S0}} \tag{2}$$

Here, L is the initial center-to-center distance between two bubbles,and R_{L0} and R_{S0} are the initial radii of the larger and smaller bubbles, respectively.

In this study, by adjusting the laser energy (including the laser energy that generates large cavitation each time and the laser energy that generates small cavitation each time) and the time interval between two pulsed lasers, two continuous pulsed lasers with a time interval are used to induce breakdown in the pure water liquid medium. The two laser pulses are sequentially delivered with an extremely short time interval (ranging from 100 ns to 4 μs in this study, negligible compared to the entire bubble pulsation cycle, causing no overall phase difference) through the same set of optical reflection focusing devices vertically into deionized water, ensuring an absolute vertical structure in the space between the two cavitation bubbles. However, the difference in laser energy affects the height of the laser focal point under the same optical reflection conditions on the same liquid surface. When the two laser pulses, which are emitted sequentially with a time interval, induce a vertical breakdown vertically into the deionized water, the plasma generated by the first breakdown causes a disturbance in the liquid layer. Subsequently, the breakdown point of the latter pulse shift upwards due to the disturbance after experiencing the time interval, thus increasing the vertical distance between the two cavitation bubbles.

Therefore, by independently adjusting the energy of the two laser pulses, the initial size of each larger and smaller bubble can be changed, thereby altering the initial size ratio S^*. Additionally, by jointly adjusting the laser energy and the time interval between the two laser pulses (ranging from 100 to 4000 ns), the vertical distance between the two cavitation bubbles can be changed, thereby altering the relative distance D^*.

According to previous studies, when the size difference between bubbles is less than 15% [10], it is defined as similar-sized bubbles. In this study, based on the initial size ratio S*, the double cavitation bubbles are categorized into three types: similar-sized doublel cavitation bubbles, different-sized double cavitation bubbles, and extremely different-sized double cavitation bubbles. Additionally, when observing the interaction phenomena of double cavitation bubbles by jointly changing the relative distance D^* between them, they are further categorized into three operating conditions based on common pulsation characteristics.

This study investigates three different operating conditions (Table 1 summarizes the initial size ratio S^* and relative distance D^* of the double cavitation bubbles in the six experimental groups for the three operating conditions, aiming to make the understanding of the operating conditions clear):

① Similar-sized double cavitation bubbles $R_{L0} \approx R_{S0}$: The definition of similar-sized double cavitation bubbles is based on the fact that the bubble size difference is less than 15% [10]. The initial size ratio S^* of this part of double cavitation bubbles is 1–1.15, and the relative distance D^* is 0–1 range.

Table 1 Summary of six sets of experimental initial size ratios S^* and relative spacing D^* for double cavitation bubbles in three types of work situations

	Similar-sized double cavitation bubbles		Different-sized double cavitation bubbles		Extremely different-sized double cavitation bubbles	
	$S^*=1.039$	$S^*=1.134$	$S^*=1.604$	$S^*=2$	$S^*=3.609$	$S^*=5.574$
D^*	0.226	0.313	1.608	1.283	2.350	2.280

② Different-sized double cavitation bubbles $R_{L0} > R_{S0}$: The initial size ratio S^* of double cavitation bubbles in this part is 1.15–3, and the relative distance D^* is in the range of 1–2.

③ Extremely different-sized double cavitation bubbles $R_{L0} \gg R_{S0}$: The initial size ratio S^* of this part of the double cavitation bubbles is 3 or above. This means that the larger bubble's initial size is at least two times greater than the smaller bubble's initial size, so it is called extremely different-sized. The relative distance D^* is in the range of 2–3.

3 Results and discussion

3.1 Interaction of similar-sized double cavitation bubbles($R_{L0} \approx R_{S0}$)

Using pulsed laser to induce breakdown in the liquid medium, multiple sets of pulsation processes for double cavitation bubbles with similar sizes were obtained. Figure 2 shows images of the interaction of a set of similar-sized double cavitation bubbles in the liquid medium. These images were captured by a high-speed camera, with each frame displaying the process starting from the generation of the plasma. The frame interval is 12 μs. The initial radii of the two cavitation bubbles are 0.995 mm and 0.958 mm, with an initial size ratio S^* of 1.039. The two bubbles are nearly equal in size, meeting the criteria for similar-sized definition. The absolute distance of the double cavitation bubbles is 0.442mm, and the relative distance D^* is 0.226. The two

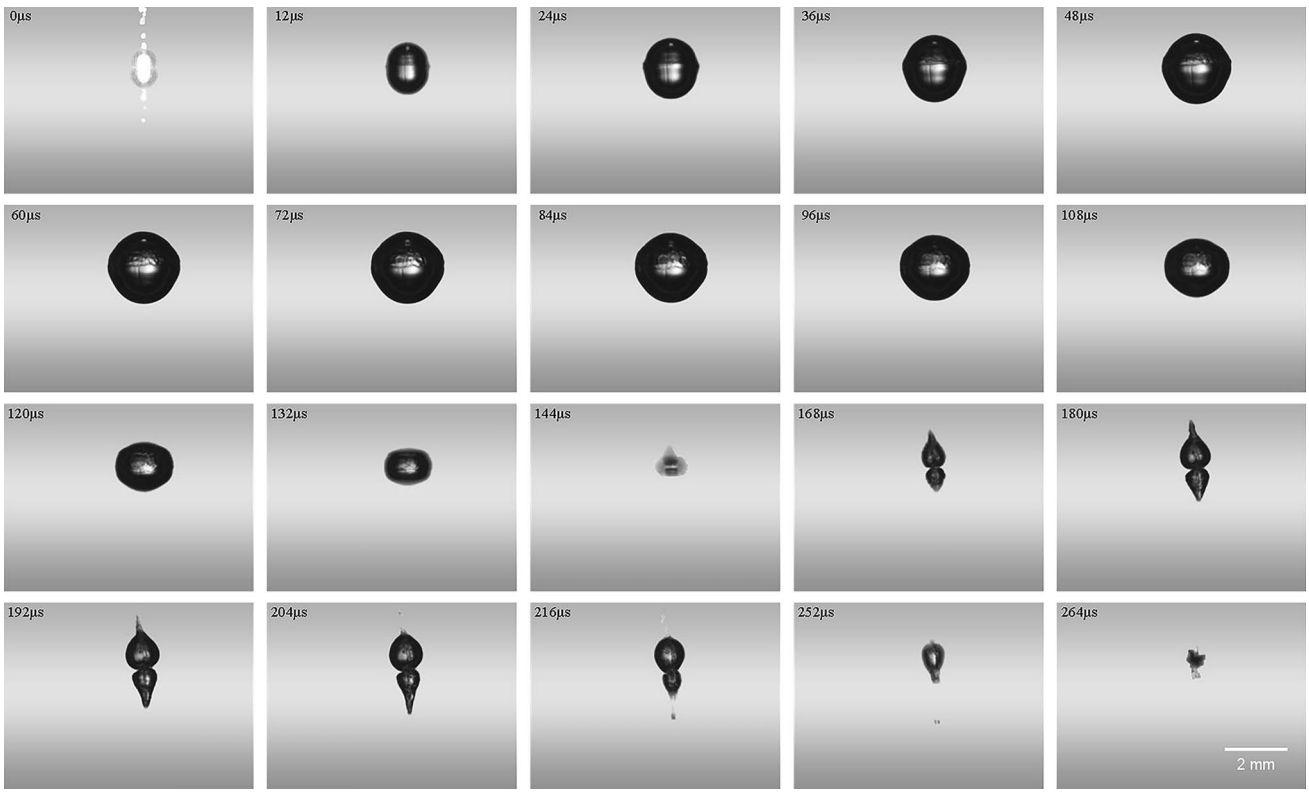

Fig. 2 Pulsation sequence diagram of vertically structured similar-sized double cavitation bubbles (I)

similar-sized cavitation bubbles formed are initially very close, exhibiting characteristics of partial fusion.The bubbles are generated and grow simultaneously, initiating fusion in the early expansion phase and gradually coalescing into a single bubble. The newly formed bubble from the fusion continues to expand until 84 μs. At $t = 96$ μs, compression of the coalesced bubble occurs. It can be visually observed in the graph that the bubble is compressed from the top and bottom towards the center. At 144 μs, the coalesced b bubble reaches its minimum compression and shows a tendency to split into two parts.After 144 μs, the coalesced bubble exhibits a separation into two parts with reverse stretching, gradually becoming more pronounced. Eventually, this leads to the micro-jet flows in opposite directions on both sides, resulting in the collapse of the bubble.

Figure 3 shows another set of images depicting the pulsation of double bubbles of similar sizes in a liquid medium. The initial radii of the two bubbles are 1.253 mm and 1.105 mm, with an initial size ratio S^* of 1.134, meeting the criteria for similar-sized definition. The absolute distance between the double cavitation bubbles is 0.737 mm, and the relative distance D^* is 0.313. The recorded process remains consistent with the overall pulsation process in Fig. 3, involving the double cavitation bubbles coalescence, expansion, flattening and compression, separation into two, stretching on both sides, and collapse due to reverse jetting. Moreover, due to a larger initial size ratio compared to Fig. 2, the simultaneous expansion and coalescence process of the double cavitation bubbles is more pronounced.

In summary, for the system of horizontally aligned double cavitation bubbles with equal sizes and in-phase behavior, the dynamic characteristics of bubble collapse are entirely consistent. Within one collapse cycle, there is an attractive force between the double cavitation bubbles, driving them closer together [17, 18] Through analysis, it is found that this also applies to vertically structured double cavitation bubbles with similar sizes. The two bubbles initially attract each other during the expansion process, so during the $t = 0$ to 60μs stage in Fig. 2, the double cavitation bubbles exhibit simultaneous expansion and fusion. After merging into a spherical shape, due to the continued attractive force between the two bubbles, the original two parts continue to squeeze towards each other, causing the merged bubble to flatten. At 84μs, the size of the merged bubble shows a shrinking trend, until 144μs when the bubble compresses to the minimum. At this point, the prototype of micro-jets stretching on both sides can be observed. The analysis suggests that after the merged bubble compresses to the minimum, an explosive shock occurs, generating a reactive force upward and downward. This rapid upward and downward reaction propels the micro-jet ejection, causing the bubble to stretch, and eventually, the two parts formed by the impact collapse due to excessive stretching and deformation.

Simultaneously, from a macroscopic perspective of the number of bubbles, the vertically arranged similar-sized double cavitation bubbles exhibit a "first merge and then separate" characteristic during the pulsation process. In other words, two bubbles merge and squeeze each other due to mutual attraction, forming a merged bubble, and then continue to squeeze and compress toward each other.Subsequently, under compression to the limit, the merged bubble collapses and explodes into two parts, and eventually, the two parts collapse due to opposing micro-jets.

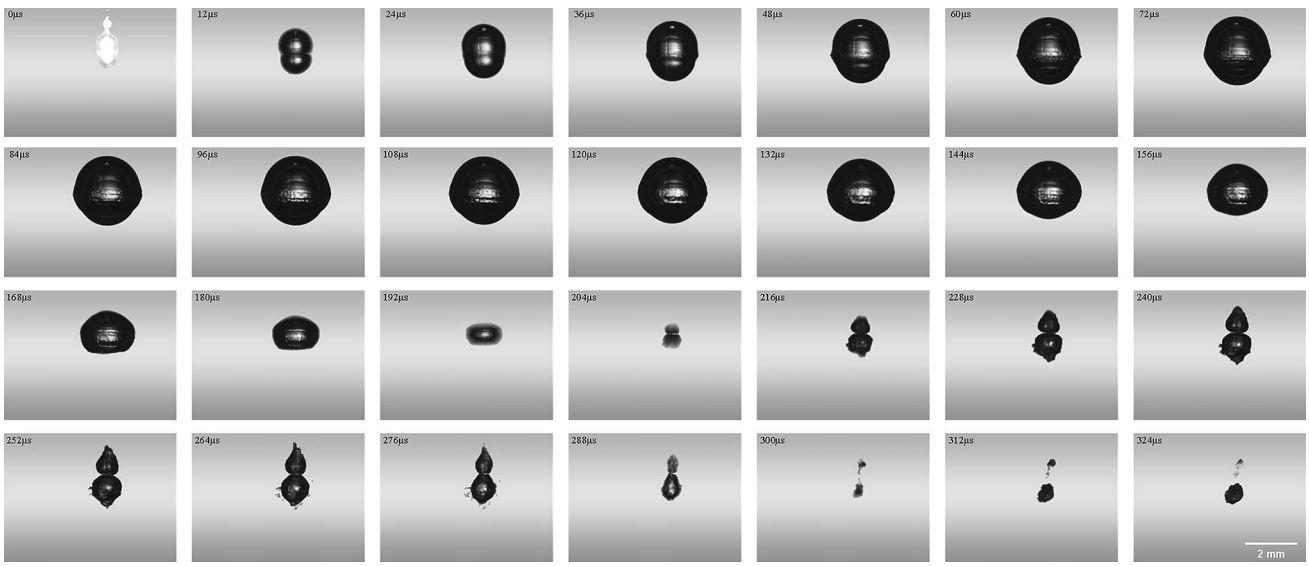

Fig. 3 Pulsation sequence diagram of vertically structured similar-sized double cavitation bubbles (II)

3.2 Interaction of different-sized double cavitation bubbles($R_{L0} > R_{S0}$)

In the experiments of pulsed laser-induced vertical double cavitation bubbles, cases of different-sized double cavitation bubbles are the most commonly observed. In this study, double cavitation bubbles with an initial size ratio (S^*) in the range of 1.15–3 are defined as different-sized double cavitation bubbles. Furthermore, the occurrence of the "slingshot effect" of double bubbles is observed within the range of initial size ratio S^* of 1.15–3 and relative distance D^* of 1–2. Figure 4 shows the vertical structure of double cavitation bubbles with large bubbles at the top and small bubbles at the bottom. Figure 5 shows the vertical structure of double cavitation bubbles with small bubbles at the top and large bubbles at the bottom.

Each set is recorded from the generation of the plasma, with a frame interval of 12 μs. In Fig. 4(a), the initial radius of the large bubble is 1.115 mm, and the initial radius of the small bubble is 0.695 mm, with an initial size ratio S^* of 1.604. The initial absolute distance between the double cavitation bubbles is 2.911 mm, and the relative distance D^* is 1.608. After the simultaneous generation of the double cavitation bubbles, they grow and expand together. The

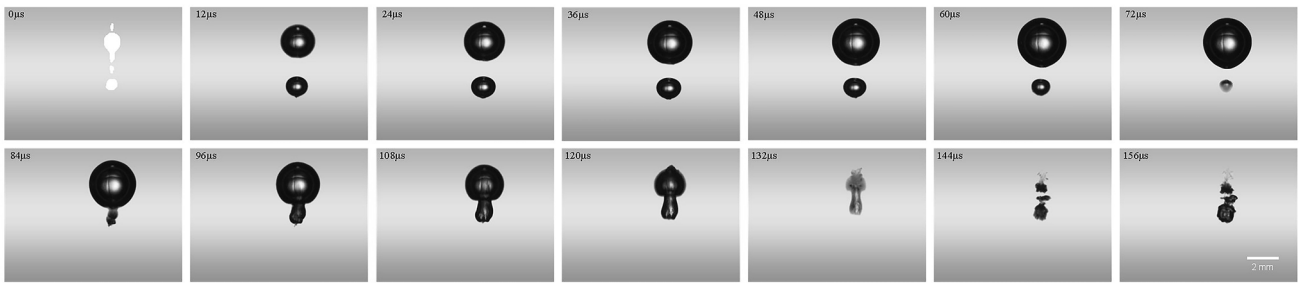

(a) Pulsation sequence diagram of vertically structured different-sized double cavitation bubbles(I)

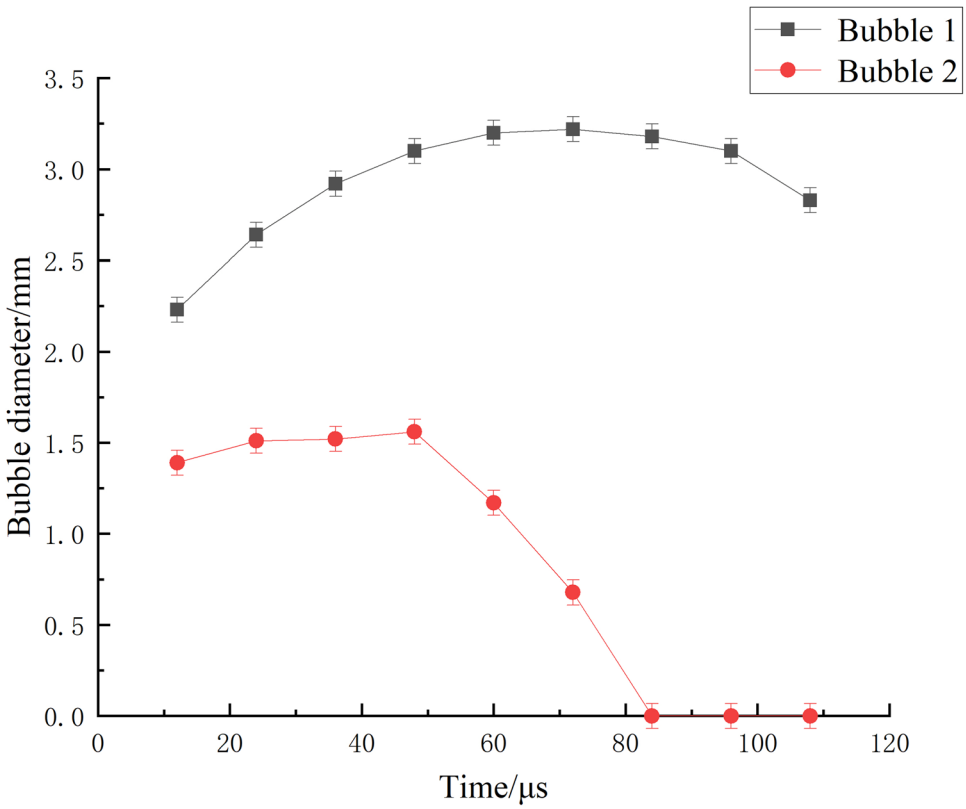

(b) Diameter curve of two cavitation bubbles with time

Fig. 4 Double cavitation bubbles evolution diagram of vertical structure with large top and small bottom

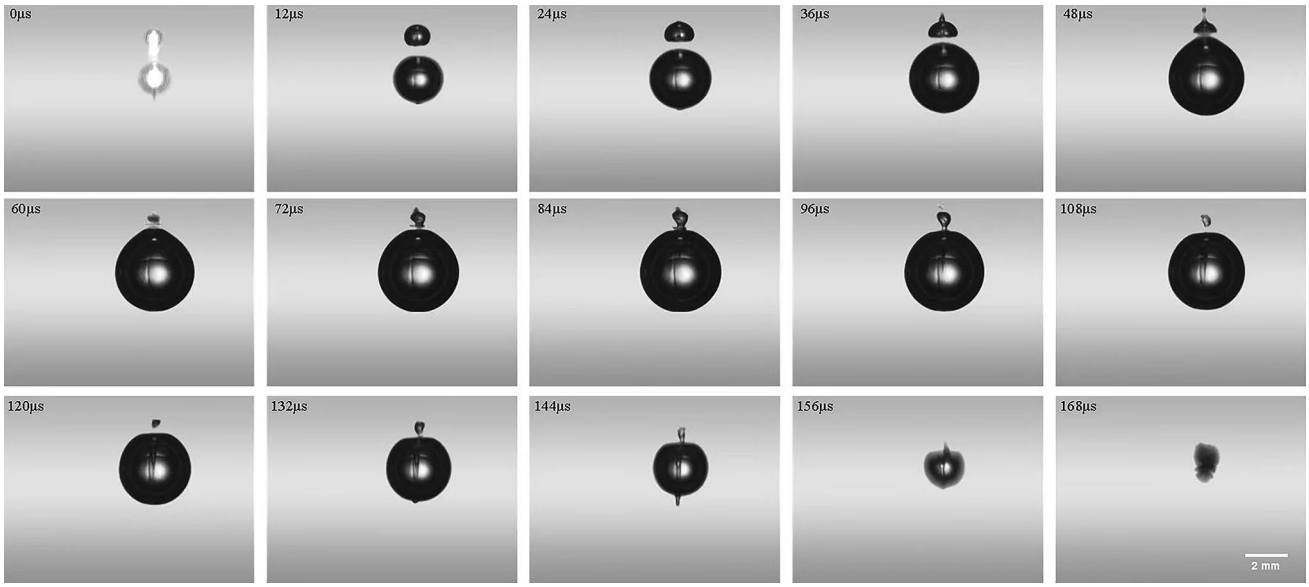

Fig. 5 Pulsation sequence diagram of vertically structured different-sized double cavitation bubbles (II)

difference is that the large bubble maintains spherical expansion from $t=0$ to 48μs, while the small bubble only maintains spherical expansion from $t=0$ to 12μs. Thereafter, it transforms into an elliptical shape at 24 μs and begins to shrink after 48 μs. At the same time, after 48μs, the large bubble exhibits outward growth in a convex shape pointing in the direction of the small bubble, losing its spherical shape. The small bubble continues its ellipsoidal contraction until it collapses (with a trend of micro-jet emission). After the collapse of the small bubble, the two undergo morphological changes again.

We analyze this process together with the diameter change curve of double cavitation bubbles with time in Fig. 4(b). Initially, from $t=0$ to 48μs, both bubble radii increase, indicating the expansion phase.During the expansion phase, two different-sized bubbles experience mutual repulsion. Consequently, the small bubble undergoes ellipsoidal expansion due to the combined effects of repulsion and its own expansion force. Meanwhile, the large bubble, possibly due to its significantly greater expansion force compared to the repulsion, maintains spherical expansion. After 48μs, the small bubble shrinks due to the repulsion from the expansion of the large bubble overpowering its own expansion force. Simultaneously, the contraction of the small bubble provides an attractive force toward the large bubble. The combination of this attraction force and the expansion force of the large bubble in the same direction leads to the subsequent outward convex growth of the large bubble. At $t=84$μs, the small bubble collapses, impacting the large bubble and causing rapid contraction. The contraction of the large bubble generates an attractive force. Therefore, at $t=96$μs, the self-shrinkage of the large bubble quickly attracts the collapsed bubble part into itself. At 108μs, a relatively large micro-jet forms, and at 120μs, the micro-jet pierces through the large bubble, leading to its collapse.

If the entire pulsation is observed with two cavitation bubbles as a whole, when the double bubbles initially stretch and expand in one direction (from the large bubble towards the small bubble), followed by a rapid contraction in the opposite direction and the ejection of a jet, the entire process resembles a slingshot launch. This phenomenon is referred to as the "slingshot effect"of the bubbles. It can be clearly seen from Fig. 5 that a clearer cavitation "slingshot effect" appears, which is mutually verified with the analysis in Fig. 4. In Fig. 5, the initial radius of the large bubble is 1.130 mm, and the initial radius of the small bubble is 0.565 mm, with an initial size ratio S^* of 2. The absolute distance between the double cavitation bubbles is 2.174 mm, and the relative distance (D^*) is 1.283. After the two bubbles are generated, they begin to expand. The large bubble maintains a spherical expansion, while the small bubble undergoes flattening with a trend of reverse jet formation.This is the result of the repulsive force generated by the expansion of the large bubble. From $t=36$μs to 60μs, the small bubble exhibits reverse jet formation due to the significant repulsive force. During this process, the small bubble shrinks while generating an attractive force on the large bubble. Under the combined action of attraction and expansion forces, the large bubble exhibits outward growth resembling a water droplet. The small bubble collapses due to the impact of the reverse micro-jet, and its collapsing shock wave affects the large bubble, causing it to shrink rapidly. The shrinkage of the large bubble quickly attracts the collapsing bubble. At $t=96$μs, it is clearly observed that the collapsing bubble

generates micro-jets directed towards the large bubble due to the attractive force. Subsequently, at $t = 108$ μs, the originally collapsed bubble undergoes a secondary collapse, and it is distinctly observed that the first micro-jet completely rushes into the large cavitation. Then the first micro-jet begins to vertically pierce the large bubble. The large bubble contracts again, attracting the micro-jet. Meanwhile, after the original collapsed bubble undergoes a secondary collapse, a second micro-jet is generated due to attraction. In the end, the entire cycle of collapse of the large bubble concludes with the penetration of the first micro-jet, reaching 168μs.

To sum up, it is found that when the initial size ratio S^* of double cavitation bubbles induced by pulse laser is in the range of 1.15–3, the relative distance D^* is observed to be roughly in the range of 1–2. Bubbles of different sizes exhibit repulsive forces during the expansion process and attractive forces during the contraction process. This results in a cyclic interplay of repulsive and attractive forces between the two bubbles. The smaller bubble, under the influence of repulsive forces, collapses and is subsequently attracted by the larger bubble, leading to the emission of micro-jets. These micro-jets pierce through the larger bubble, causing its collapse. At the same time, this process is prone to the so-called cavitation "slingshot effect".

3.3 Interaction of extremely different-sized double cavitation bubbles($R_{L0} \gg R_{S0}$)

In the experiments inducing double cavitation bubbles with pulsed laser, double bubbles with an initial size ratio S^* greater than 3 were observed. Under this condition, the size of the larger bubble is at least twice that of the smaller bubble, defining them as extremely different-sized double cavitation bubbles. Furthermore, it was observed that extremely different-sized double cavitation bubbles generally have a considerable distance between them, with the observed relative distance D^* falling within the range of 2–3. Figure 6 shows the vertical structure with large bubbles on top and small bubbles on the bottom. Figure 7 shows the vertical structure with small bubbles on top and big bubbles on the bottom.

In Fig. 6(a), the initial radius of the large bubble is 0.985 mm, and the initial radius of the small bubble is 0.321 mm. The initial size ratio of the two bubbles is 3.069. The absolute distance between the double cavitation bubbles is 3.058 mm, and the relative distance is 2.350. Figure 6 depicts a vertical configuration with the larger bubble positioned above and the smaller bubble positioned below. After the generation of the two bubbles, the large bubble maintains spherical expansion, while the small bubble exhibits a micro-jet in the opposite direction and collapses. Subsequently, the large bubble continues to expand, contract, and collapse in a spherical manner. Combined with the analysis of the change curve of large and small cavitation diameters over time,the large bubble still exerts a repulsive force on the small bubble during the expansion process. Therefore, the small bubble undergoes flattening and compression at $t = 24$μs and exhibits a micro-jet in the opposite direction at $t = 36$μs. According to previous research, small cavitation bubbles also generate force on large cavitation bubbles during the shrinkage process. However, this force may be weakened due to (1) the substantial distance and significant relative distance between the bubbles, leading to a reduction in the effectiveness of force due to the weakening resistance of the liquid medium [19]; (2)the interaction force between cavitation bubbles being dependent on the size of the cavitation bubbles that generate and withstand the cavitation bubbles. In essence, larger bubble generate more substantial fluctuating forces, while smaller bubble experience a greater impact from the fluctuating force.On the contrary, the effect of the fluctuating force on the cavitation bubble will be smaller. Therefore, the large bubble is almost unaffected by the force generated by the small bubble and maintains its spherical expansion. From a macroscopic perspective, the pulsation process of the large bubble is essentially consistent with the pulsation process of a single cavitation bubble in a free field [20, 21].

In Fig. 7, the initial radius of the large bubble is 1.165 mm, the initial radius of the small bubble is 0.209 mm. The initial size ratio of the two bubbles is 5.574. The absolute distance between the two bubbles is 3.132 mm, and the relative distance is 2.280. Figure 7 depicts a vertical structure with the small bubble on top and the large bubble on the bottom. The pulsation characteristics of the group in Fig. 7 remain consistent with the pulsation characteristics of the vertical structure with the small bubble on top and the large bubble on the bottom. At $t = 12$μs, the small bubble shows a tendency to develop into an ellipsoidal shape, and at 36μs, a reverse micro-jet appears. This is all due to the repulsive force caused by the expansion of the large bubble. The expansion, shrinkage, and micro-jet emission of the small bubble have little effect on the large bubble due to the large distance and significantly greater size, maintaining the complete spherical process of expansion, shrinkage, and collapse.

In summary, it is observed that the relative distance D^* of the double bubbles is in the range of 2–3. During the expansion of the large bubble, it generates repulsive forces on the small bubble. Moreover, due to the significantly large initial size ratio, the repulsive force on the small bubble is particularly pronounced. On a macroscopic scale, in the pulsation process of extremely different-sized double bubbles, the growth of the large bubble inhibits that of the small bubble. The pulsation characteristics of the large bubble are essentially consistent with those of a single bubble in a free field.

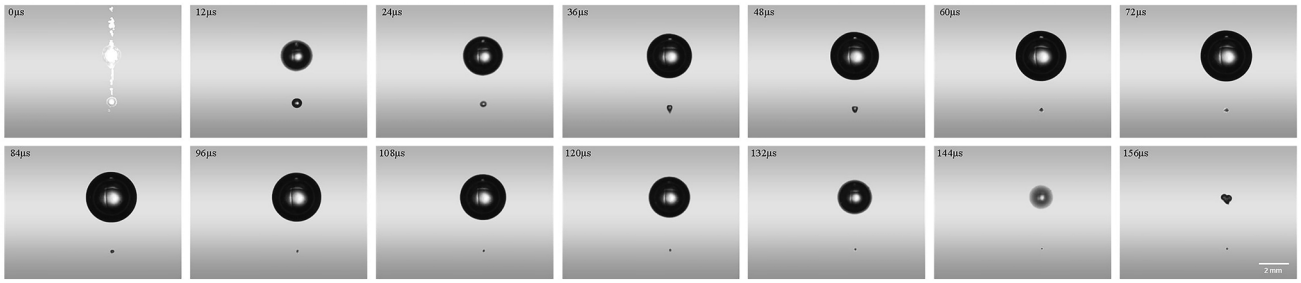

(a)Pulsation sequence diagram of vertically structured extremely different-sized double cavitation bubbles

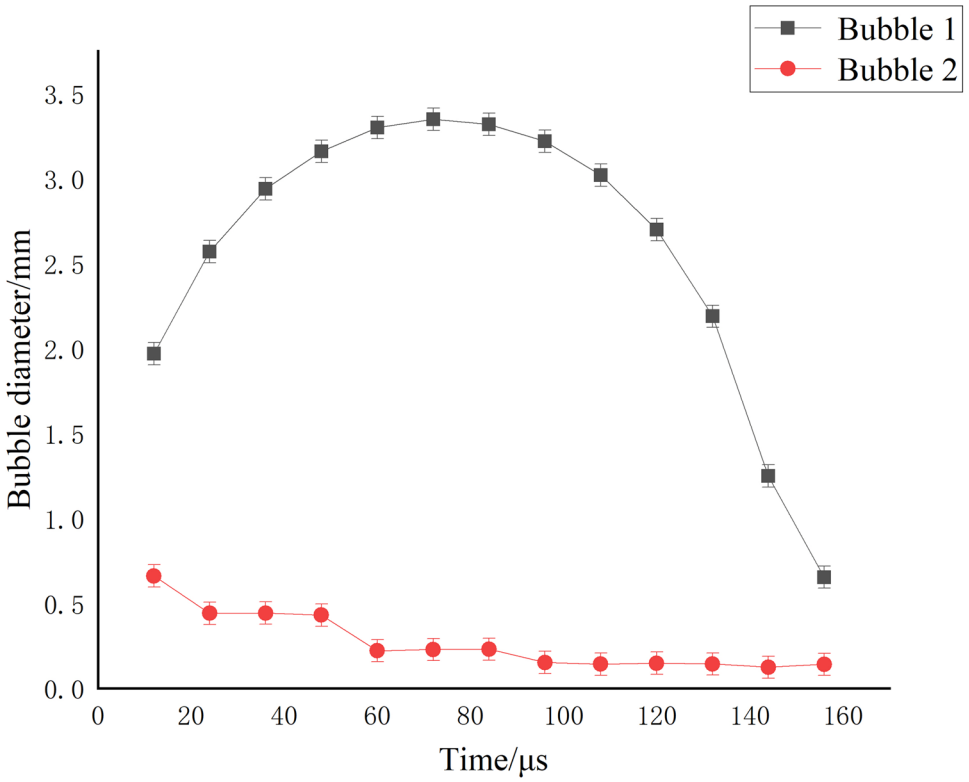

(b) Diameter curve of the two cavitation bubbles with time

Fig. 6 Double cavitation bubbles evolution diagram of vertical structure with large top and small bottom

Moreover, the up and down order of the large and small cavitation bubbles in the vertical structure does not affect the overall pulsation characteristics.

4 Conclusion

This study employs the pulsed laser-induced cavitation method to to induce the generation of double cavitation bubbles and simultaneously utilizes high-speed photography technology to investigate the pulsation process of three size categories of double cavitation bubbles in a vertically arranged structure. The research results show that in the interaction process of vertically arranged double cavitation bubbles:

(1) Similar-sized double cavitation bubbles mutually attract and merge, followed by mutual compression, reaching a limit, and then exhibiting reverse stretching and jetting, presenting a 'merge before separation' characteristic.
(2) In the pulsation process of different-sized double cavitation bubbles, the expansion of one bubble generates repulsive forces against the other, while the contraction exerts attractive forces. This leads to a series of com-

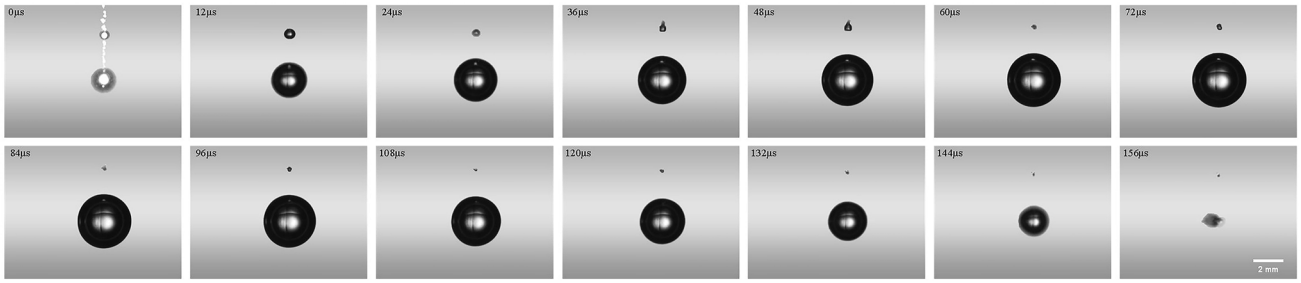

(a) Pulsation sequence diagram of vertically structured extremely different-sized double cavitation bubbles

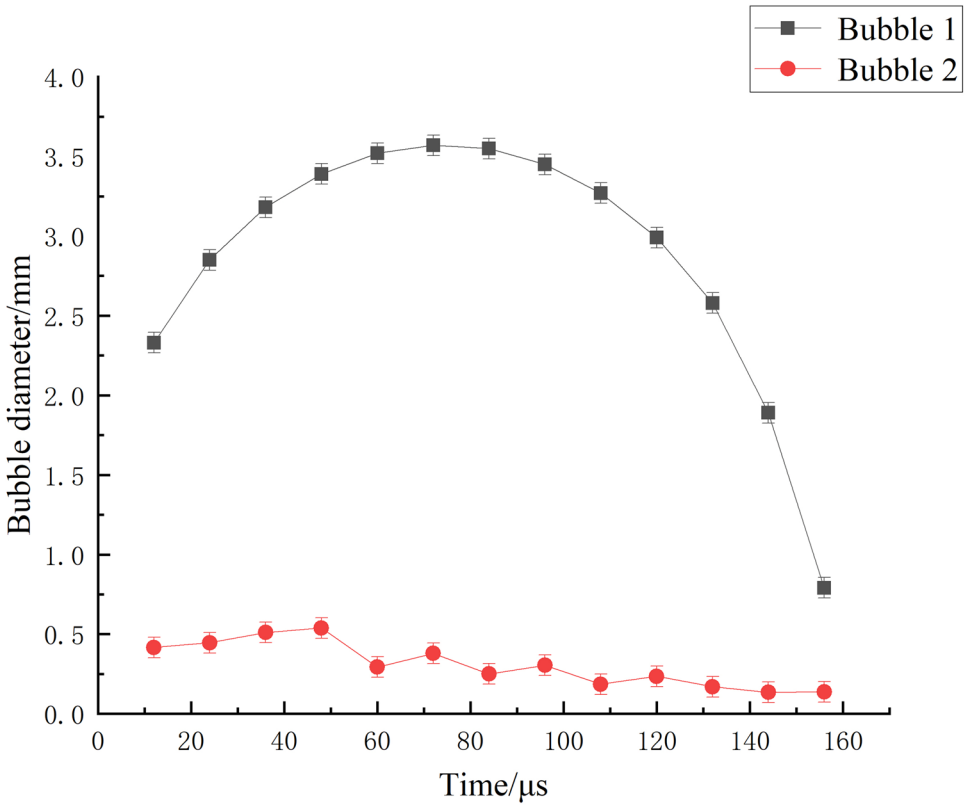

(b) Diameter curve of the two cavitation bubbles with time

Fig. 7 Double cavitation bubbles evolution diagram of vertical structure with small top and large bottom

plex phenomena, and under certain conditions, it can result in the formation of a "slingshot effect".The process has certain similarities with the pulsation process of horizontally arranged anti-phase double cavitation bubbles [12].

(3) In the pulsation process of extremely different-sized double cavitation bubbles, the growth of the large bubble inhibits the growth of the small bubble, leading to the reverse jet emission and collapse of the small bubble. The pulsation characteristics of the large bubble are essentially consistent with those of a single cavitation bubble in a free field [20, 21].

Although this study has conducted a comprehensive analysis of the pulsation process of double bubbles in a vertical arrangement, further exploration can be pursued in the later stages by altering the medium environment of vertically structured double cavitation bubbles and quantifying their mutual interactions.

Acknowledgements This document presents the results of the research project funded by the Ministry of Education Chunhui Project (HZKY20220606-202201390), Civil Aviation University of China Postgraduate Scientific Research Innovation Project-Aviation Special Project (2022YJS069), and Civil Aviation University of China Virtual Simulation Experiment Teaching Construction Project(XF2022002).

Authors contributions All authors contributed to the study conception and design. Qingmiao Ding and Yunlong Shan wrote the main manuscript text. Material preparation, data collection and analysis were performed by Yanyu Cui, Xiaoman Li, Junguo Ni and Junda Lv. All authors commented on previous versions of the manuscript. All authors read, reviewed and approved the final manuscript.

Funding This document presents the results of the research project funded by the Ministry of Education Chunhui Project (HZKY20220606-202201390), Civil Aviation University of China Postgraduate Scientific Research Innovation Project-Aviation Special Project (2022YJS069), and Civil Aviation University of China Virtual Simulation Experiment Teaching Construction Project(XF2022002).

Data availability The data that support the findings of this study are available on request from the corresponding author,, Yanyu Cui, upon reasonable request.

Declarations

Conflict of Interests The authors have no competing interests to declare that are relevant to the content of this article.

Ethical Approval The study is not applicable for both human and/ or animal studies and complies with ethical standards.

References

1. X.X. Wu, H.Y. Zhang, K.J. Ma, Research progresses of movement characteristics of ultrasonic cavitation bubbles. Journal of Applied Acoustics **31**(06), 416–422 (2012)
2. C.L. Kling, F.G. Hammitt, A photographic study of spark-induced cavitation bubble collapse. Journal of Fluids Engi-neering **94**(4), 825–833 (1972)
3. Y.M. Shi, F.H. Ma, X.J. Tu, Research and Application of Laser-induced Cavitation Technology. Science & Technology Information **21**(13), 68–71 (2023)
4. T.M. Mitchell, F.G. Hammitt, Asymmetric Cavitation bubble collapse[J]. J. Fluids Eng. **95**(1), 29–37 (1973)
5. W. Lauterborn, W. Hentschel, Cavitation bubble dynamics studied by high speed photography and holography: part one. Ultrasonics **23**(6), 260–268 (1985)
6. W. Lauterborn, W. Hentschel, Cavitation bubble dynamics studied by high speed photography and holography: part two. Ultrasonics **24**(2), 59–65 (1986)
7. Y. Tomita, A. Shima, K. Sato, Dynamic behavior of two-laser-induced bubbles in water. ApplPhys **57**(3), 234–236 (1990)
8. S.W. Fong, D. Adhikari, E. Klaseboer, B.C. Khoo, Interactions of multiple spark-generated bubbles with phase differences. Exp. Fluids **46**(4), 705–724 (2009)
9. P.A. Quinto-Su, C.D. Ohl, Interaction between two laser-induced cavitation bubbles in a quasi-two-dimensional geometry. J. Fluid Mech. **633**(633), 425–435 (2009)
10. L. W. Chew, E. Klaseboer, S. W. Ohl, B. C. Khoo: Interaction of two differently sized oscillating bubbles in a free field. Physical Review E 84(6):066307(2011).
11. C.T. Hsiao, J.K. Choi, S. Singh, G.L. Chahine, T.A. Hay, Y.A. Ilinskii, E.A. Zabolotskaya, M.F. Hamilton, G. Sankin, F. Yuan, P. Zhong, Modelling single-and tandem-bubble dynamics between two parallel plates for biomedical applications. J. Fluid Mech. **716**, 137–170 (2013)
12. B. Han, K. Köhler, K. Jungnickel, R. Mettin, W. Lauterborn, A. Vogel, Dynamics of laser-induced bubble pairs. J. Fluid Mech. **771**, 706–742 (2015)
13. L.B. Tao, A three-dimensional modeling for coalescence of multiple cavitation bubbles near a rigid wall. Phys. Fluids **31**(6), 062107–062107 (2019)
14. V. Robles, E. Gutierrez-Herrera, L. F. Devia-Cruz, D. Banks, S. Camacho-Lopez, G. Aguilar: Soft material perforation via double-bubble laser-induced cavitation microjets. Physics of Fluids 32(4): 042005(2020).
15. L. Fu, P. Wang, S.J. Wang, J. Xin, L.W. Zhang, Dynamics of Bubble Pairs in Water Induced by Focused Nanosecond Laser Pulse. Chin. J. Lasers **49**(4), 0407001–0407001 (2022)
16. M. Dan, J. D. N. Cheeke, L. Kondic: Ambient pressure effect on single-bubble sonoluminescence[J]. Physical Review Letters 83(9): 1870(1999).
17. Y.Q. Tong, C. Wang, S.Q. Yuan, K.G. Han, X.M. Chen, N. Yang, X.D. Ren, Compound strengthening and dynamic characteristics of laser-induced double bubbles. Opt. Laser Technol. **113**, 310–316 (2019)
18. F.C. Li, J. Cai, X.L. Huai, B. Liu, Interaction Mechanism of Double Bubbles in Hydrodynamic Cavitation. J. Therm. Sci. **03**, 242–249 (2013)
19. H. Nazari-Mahroo, K. Pasandideh, H.A. Navid, R. Sadighi-Bonabi, Influence of liquid density variation on the bubble and gas dynamics of a single acoustic cavitation bubble. Ultrasonics **102**, 106034 (2020)
20. Z.W. Jia, D. Li, Y. Tian, H.P. Pan, Q. Zhong, Z.F. Yao, Y. Lu, J.J. Guo, R. Zheng, Early dynamics of laser-induced plasma and cavitation bubble in water. Spectrochim. Acta, Part B **206**, 106713 (2023)
21. O. Supponen, D. Obreschkow, M. Tinguely, P. Kobel, N. Dorsaz, M. Farhat, Scaling laws for jets of single cavitation bubbles. J. Fluid Mech. **802**, 263–293 (2016)